PROCEEDINGS
SECOND WORKSHOP
GEOTHERMAL RESERVOIR ENGINEERING
December 1-3, 1976

Paul Kruger and Henry J. Ramey, Jr., Editors
Stanford Geothermal Program
Workshop Report SGP-TR-20*

DISCLAIMER

DISCLAIMER

Portions of this document may be illegible in electronic image products. Images are produced from the best available original document.

A MODEL OF THE HYDROTHERMAL SYSTEM
OF LONG VALLEY CALDERA, CALIFORNIA

Michael Sorey
U. S. Geological Survey
Water Resources Division
345 Middlefield Road
Menlo Park, CA 94025

Long Valley caldera, an elliptical depression covering 450 km^2 on the eastern front of the Sierra Nevada in east-central California (Fig. 1), contains a hot-water convection system with numerous hot springs and measured and estimated aquifer temperatures at depth of 180°C-280°C. In this study, the results of previous geologic, geophysical, geochemical, and hydrologic investigations of the Long Valley area have been synthesized to develop a generalized conceptual and mathematical model which describes the natural conditions of heat and fluid flow in the hydrothermal system. Because only one deep drill-hole (2 km) has thus far been completed within the caldera, this model must be considered speculative in detail, although its gross features are consistent with known constraints. Details of the work discussed in this summary will be published as a U.S.G.S. open-file report in February, 1977.

Conceptual Model

As illustrated in Figure 2, the conceptual model is three-dimensional, including the area within the topographic boundary of the caldera floor, and extending to a depth of 6 km. For numerical simulation the caldera rocks are divided into five horizontal layers, corresponding in composition and depth to the major rock units identified by the seismic refraction and geologic studies (Hill, 1976; Bailey and others, 1976), and calculations of average depths of fill (F. H. Olmsted, written communication, 1976). Of these, the upper layer, which is 1-km thick, corresponds to the post-caldera sedimentary (glacial, alluvial, and lacustrine) and volcanic (flows and tuffs) rocks and contains the shallow, cold ground-water system. Layer 2, 1-km thick, corresponds to the densely welded Bishop Tuff, a rhyolitic ash flow that erupted 0.7 m.y. ago during caldera formation. Layer 3 includes welded Bishop Tuff, the pre-caldera Glass Mountain Rhyolite, and some granitic and metamorphic basement rocks. Geophysical and geologic studies show that the densely welded tuff forms a continuous layer over the area of the caldera with an average thickness of 1.4 km. It is likely that the welded tuff has retained significant permeability after fracturing. In the conceptual model, a deep, hot ground-water system, i.e. the hydrothermal reservoir, is assumed to occur in layers 2 and 3. Layers 4 and 5 correspond to pre-caldera

basement rocks, which are assumed impermeable but thermally conductive.
Two layers were used in this depth interval (3-6 km) to allow more
accurate numerical heat flow simulation. The presence of magma below
6 km in the western part of the caldera, which is suggested by seismic,
teleseismic, and heat-flow studies, is simulated by a constant (with
time) but areally varied temperature distribution at the base of the
model.

Hydraulic and thermal properties used in the model are listed in
Table 1.

Table 1.--Hydraulic and thermal properties for Long Valley model.

Layer	Thermal conductivities $mcal/(s\ ^{\circ}C\ cm)$	Heat capacity $cal/^{\circ}C\ cm^3)$	Intrinsic permeability $m^2 \times 10^{-12}$	Vertical compressibility m^2/N	Porosity
1	2	0.54 - 0.58	0	10^{-9}	0.35
2	5	0.54 - 0.58	0.03 - 0.35	10^{-10}	0.10
3	5	0.54 - 0.58	0.03 - 0.35	10^{-10}	0.05
4	6	0.54 - 0.58	0	10^{-10}	0.05
5	6	0.54 - 0.58	0	10^{-10}	0.05

Layer 1 is considered as an impermeable cap except along parts of
the caldera rim, where recharging ground water moves downward along
the ring fault, and in the Hot Creek gorge area, where hot water
flows upward along faults to discharge in the gorge springs. Ground-
water flow is from the higher altitudes along the west and northeast
rims to discharge areas at lower altitudes in Hot Creek gorge and at
depth through the southeast rim of the caldera. Additional driving
force causing flow is provided by density differences between hot
and cold parts of the flow system. The effective reservoir trans-
missivity was evaluated by specifying pressures based on water
table altitudes in recharge and discharge areas and adjusting the
reservoir permeability distribution to yield the desired mass flux
of water.

Numerical Simulation

To permit numerical simulation of heat and fluid flow, each
layer of the model is subdivided into 82 grid blocks or nodes along
land-net lines (Fig. 3). Finer nodal spacing is used near the dis-

charge areas. Hot water is assumed to discharge only over the sur-
face of the node that includes the springs in Hot Creek gorge, in
T3S/R28E-S25, and through the southeast rim as indicated in Figure 3.
Only minor differences in computed distributions of pressure and
temperature would be expected if a more detailed distribution of
hot-water discharge were modeled, because approximately 80 percent
of the surface discharge from the thermal reservoir is through the
springs in the gorge (Sorey and Lewis, 1976).

The equations and solution procedure used in this study are
described in detail by Sorey (1975). The flow equation is

$$\nabla \cdot \left[\rho \frac{k}{\mu} (\nabla P - \rho \bar{g}) \right] = C \frac{\partial P}{\partial t} \qquad (1)$$

where

ρ	=	fluid density
k	=	intrinsic permeability
μ	=	dynamic viscosity
P	=	fluid pressure
$\bar{g}$	=	gravitational acceleration vector
C	=	fluid-rock compressibility
t	=	time

Equation 1 is based on conservation of mass and Darcy's law for non-
isothermal fluid flow in porous media. An assumption inherent in this
formulation is that fluid flow in the hydrothermal system, although
probably controlled locally by permeable zones along faults, can
best be described in large scale as flow in a porous medium in which
permeability is distributed effectively throughout.

The energy equation is

$$\nabla \cdot [K_m \nabla T] - \rho c \bar{v} \cdot \nabla T = (\rho c)' \frac{\partial T}{\partial t} \qquad (2)$$

where

K_m	=	rock-fluid thermal conductivity
T	=	rock-fluid temperature
$\bar{v}$	=	Darcy velocity vector
c	=	fluid specific heat at constant volume
$(\rho c)'$	=	rock-fluid heat capacity

Equation (2) accounts for conductive and convective transfer of heat
under steady-state and transient conditions. We assume that thermal
equilibrium exists between fluid and solid phases at points of con-
tact and that heat transfer by hydrodynamic dispersion can be neg-
lected in the type of problem considered here (Mercer and others,
1975, p. 2618). Temperature-dependent parameters, μ and c, in
Eq. (3) were evaluated from tabulated data (Dorsey, 1968).

The equation of state relating fluid density to temperature is

$$\rho = \rho_o \left[1 - \beta(T-T_o) - \gamma(T-T_o)^2\right] \qquad (3)$$

where

ρ_o = fluid density at reference temperature T_o

β = thermal expansivity

γ = coefficient for second order fit

Density variations with pressure are neglected.

Simultaneous solutions to the flow and energy equations were obtained by an integrated finite-difference method involving iterative solutions at selected time steps for pressure, temperature, and velocity fields. This numerical procedure offers considerable advantages over standard finite-difference methods in terms of reduced computing times and nodal requirements (Narasimhan and Witherspoon, 1976). The time step used to solve the energy equation is continuously increased by a factor between 1 and 2, with the limitation that the maximum change in nodal temperatures per time step be less than about 10 percent of the maximum total change expected in the system. Because the response times for pressure changes are much smaller than for temperature changes, the flow system essentially equilibrates to a quasi-steady state within each thermal time step. For a simulation period of 35,000 years, approximately 50 thermal time steps were used; for a 350,000 year simulation, approximately 70 time steps were required.

Hydraulic Characteristics

Locations of the principal faults within the caldera, most of which are high angle, normal faults, are also shown in Figure 3. Fractures in the welded tuff associated with these and other faults not delineated at the land surface are considered to provide the major channels for flow in the hydrothermal system. The apparent lack of faulting in the eastern part of the caldera (with the exception of the ring fracture) need not preclude permeable zones in that area which could also occur in brecciated zones between the two major cooling units in the Bishop Tuff (Sheridan, 1968).

Values of intrinsic permeability obtained from the model for a 1-km thick reservoir with a mass flux of 250 kg/s (based on geochemical mixing models and boron discharge into Lake Crowley; Sorey and Lewis, 1976) are listed in Table 2. Interestingly, the Long Valley results of 30-50 millidarcys are within a factor of 3 of the value used by Mercer, Pinder, and Donaldson (1975) for the fractured volcanics of the Wairora aquifer at Wairakei, New Zealand.

Table 2. Intrinsic-permeability data from Long Valley model
and other studies.

Data source	Reservoir thickness (km)	Permeability $(\times 10^{-15} m^2)$
Long Valley model	I	30 – 50[1]
Wairakei model [2]	0.4 – 0.85	100
Long Valley cores [3]	---	0.0005 – 180.
NTS ash flow tuffs [4]	---	0.04 – 10.
NTS welded tuff [5] (fractured)	0.05 – 0.2	5,000 – 30,000

[1] Range for two possible cases of reservoir permeability distribution.

[2] Wairora aquifer consisting of pumice breccia and vitric tuffs as modeled by Mercer and others (1975).

[3] Data for cores of altered rock, flow rocks, and non-welded tuffs.

[4] Oak Springs Formation (Keller, 1960).

[5] Winograd and others (1971).

Comparisons with measurements on Long Valley cores, and well tests and cores at the Nevada Test Site indicate that the permeability values obtained from the model represent an integration of the effects of fracture permeability over the volume of reservoir rock.

Equivalent of "cold water" hydraulic heads from the model simulations at each node were computed using the relationship

$$H_o = P/(\rho_o g) + Z \qquad (5)$$

where ρ_o = fluid density at reference temperature (10^oC) and Z = altitude of node above sea level. An example of the resultant head distribution, in layer 2 at 1.5 km depth as seen in Figure 4, shows the predominant eastward flow toward the Hot Creek gorge area and the effects of recharge from the Glass Mountain area. The existence of deep recharge along the northeastern rim is suggested in part by the results of a 2-km deep test hole recently drilled by private industry 3 km east of Hot Creek gorge, which encountered relatively cool ground-water temperatures within the Bishop Tuff.

Thermal Characteristics

The Long Valley model is constrained by estimates of the natural heat discharge from the caldera. From spring measurements and temperature profiles in wells, the total heat discharge is estimated to be 6.9×10^7 cal/s. Applications of geochemical mixing models indicate that 190-300 kg/s of water at $210^{\circ}C-282^{\circ}C$ discharges upward from the reservoir toward the hot springs, with the highest estimated reservoir temperature corresponding to the lowest mass flux. The model was used to evaluate the depths of fluid circulation for which an underlying magma chamber could supply the required heat flow, equivalent to an average of 15 HFU over the area of the caldera, for various periods of time. The initial thermal condition was the temperature distribution at steady state in the absence of fluid flow.

Studies of saline deposits in Searles Lake, downdrainage from Long Valley (Smith, 1976), indicate that present-day hot spring discharge in the caldera has persisted for only 30,000-40,000 years. Model simulations of heat and fluid flow for a period of 35,000 years show that present-day heat discharge could have been sustained for this period by a magma chamber at 6 km with fluid circulation to 1.5-2.5 km. As shown in Figures 5 and 6, simulated reservoir temperatures at a depth of 1.5 km under the Hot Creek gorge area are near $200^{\circ}C$ after 35,000 years with a hot spring discharge of 250 kg/s. Cooler temperatures east of Hot Creek, resulting from recharge along the northeast rim, are consistent with the results reported for the deep test hole.

In contrast, Bailey, Dalrymple, and Lanphere (1976) find evidence of extensive hydrothermal alteration 0.3 m.y. ago which appears to be related to the main magma chamber rather than to the post-caldera eruptive volcanic rocks. Simulation of hot-spring discharge for periods much greater than 35,000 years produces maximum reservoir temperatures significantly cooler than the previous results. Correspondingly, deeper levels of circulation are required to sustain heat flow and reservoir temperatures above $200^{\circ}C$.

In Figure 7, reservoir temperatures under the gorge are plotted as functions of time for two cases of reservoir depth. The initial increase in reservoir temperatures prior to about 10,000 years is due to the arrival of hotter water from the west. Calculation of average ground-water travel times from recharge to discharge areas, based on the time at which reservoir temperature under the gorge begins to decline rapidly (10,000 years), yield values near 2,000 years for a 1-km thick reservoir. Simulation of present-day hot spring discharge for periods greater than about 300,000 years, after which time the system has essentially reached steady state, shows that even for the 2-3-km deep reservoir discharge temperatures fall well below $200^{\circ}C$. The results of these and other simulations with the model indicate that circulation to depths of 4-5 km would be required to sustain present-day thermal conditions over periods of 300,000 years.

Because permeable channels in the basement rocks are unlikely to exist at these depths and in view of the diverse indications of the age of hot spring activity noted above, an alternative hypothesis that discharge from the hydrothermal system has been intermittent in character is preferred. Significant periods of inactivity could have resulted from climatic variations and self-sealing processes which are in evidence today. These possibilities and the adequacy of the simplified hydrothermal model analyzed in this study can only be evaluated by deep drilling in the western part of the caldera.

Under the eastern two-fifths of the caldera, reservoir temperatures measured in the deep test hole and simulated temperatures from the model would seem to preclude the possibility of energy development east of Hot Creek. However, the significance of this area may be its potential contribution of relatively cold ground water to high-enthalpy fluid production from beneath the resurgent dome in the west-central part of the caldera, and (or) its potential for reinjection of hydrothermal fluids. The model analyzed in this study has helped to quantify the relationships between heat and fluid flow and the hydraulic characteristics of the hydrothermal system. Incorporation of additional detail from deep and shallow drilling would enable the model to be used to analyze the potential for, and the effects of, energy development in the Long Valley caldera.

Selected References

Bailey, R.A., Dalrymple, G.B., and Lanphere, M.A., 1976, Volcanism, structure, and geochronology of Long Valley caldera, Mono County, California, Jour. Geophys. Research, v. 81, no. 5, p. 725-744.

Dorsey, N.E., 1968, Properties of ordinary water-substance, Hafner Publishing Co., New York.

Hill, D.P., 1976, Structure of Long Valley caldera, California from a seismic refraction experiment, Jour. Geophys. Research, v. 81, no. 5.

Keller, G.V., 1960, Physical properties of tuffs of the Oak Spring Formation, Nevada, U.S. Geol. Survey Prof. Paper 400-B, p. 396-400.

Lewis, R.E., 1974, Data on wells, springs, and thermal springs in Long Valley, Mono County, California, U.S. Geol. Survey open-file rept. 52 p.

Mercer, J.W., Pinder, G.F., and Donaldson, I.G., 1975, A Galerkin finite-element analysis of the hydrothermal system at Wairakei, New Zealand, Jour. Geophys. Research, v. 80, no. 17, p. 2608-2621.

Narashimhan, T.N., and Witherspoon, P.A., 1976, An integrated finite difference method for analyzing fluid flow in porous media, Water Resources Research, v. 12, no. 1, p. 57-64.

Sheridan, M.F., 1968, Double cooling-unit nature of the Bishop Tuff in Owens Gorge, California (abs), Geol. Soc. America Spec. Paper 115, p. 351.

Smith, G.I., 1976, Origin of lithium and other components in the Searles Lake evaporites, California, in Lithium resources and requirements by the year 2000, U.S. Geol. Survey Prof. Paper 1005, ed. by J. D. Vine, p. 92-103.

Sorey, M.L., 1975, Numerical modeling of liquid geothermal systems, U.S. Geol. Survey open-file rept. 75-613, 66 p.

Sorey, M.L., and Lewis, R.E., 1976, Convective heat flow from hot springs in the Long Valley caldera, Mono County, California, Jour. Geophys. Research, v. 81, no. 5, p. 785-791.

Winograd, I.J., Thordarson, W., and Young, R.A., 1971, Hydrology of the Nevada Test Site and vicinity, U.S. Geol. Survey open-file rept., 429 p.
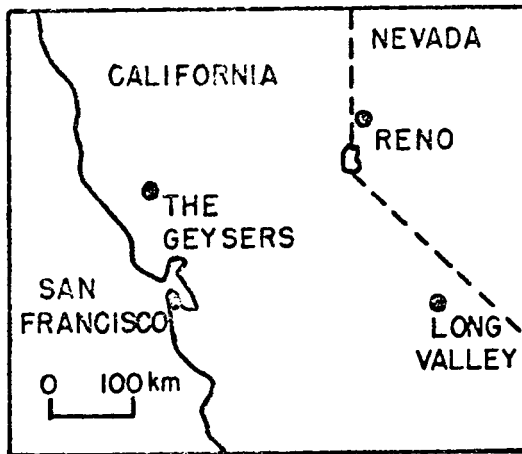
Figure 1. Map showing location of Long Valley and
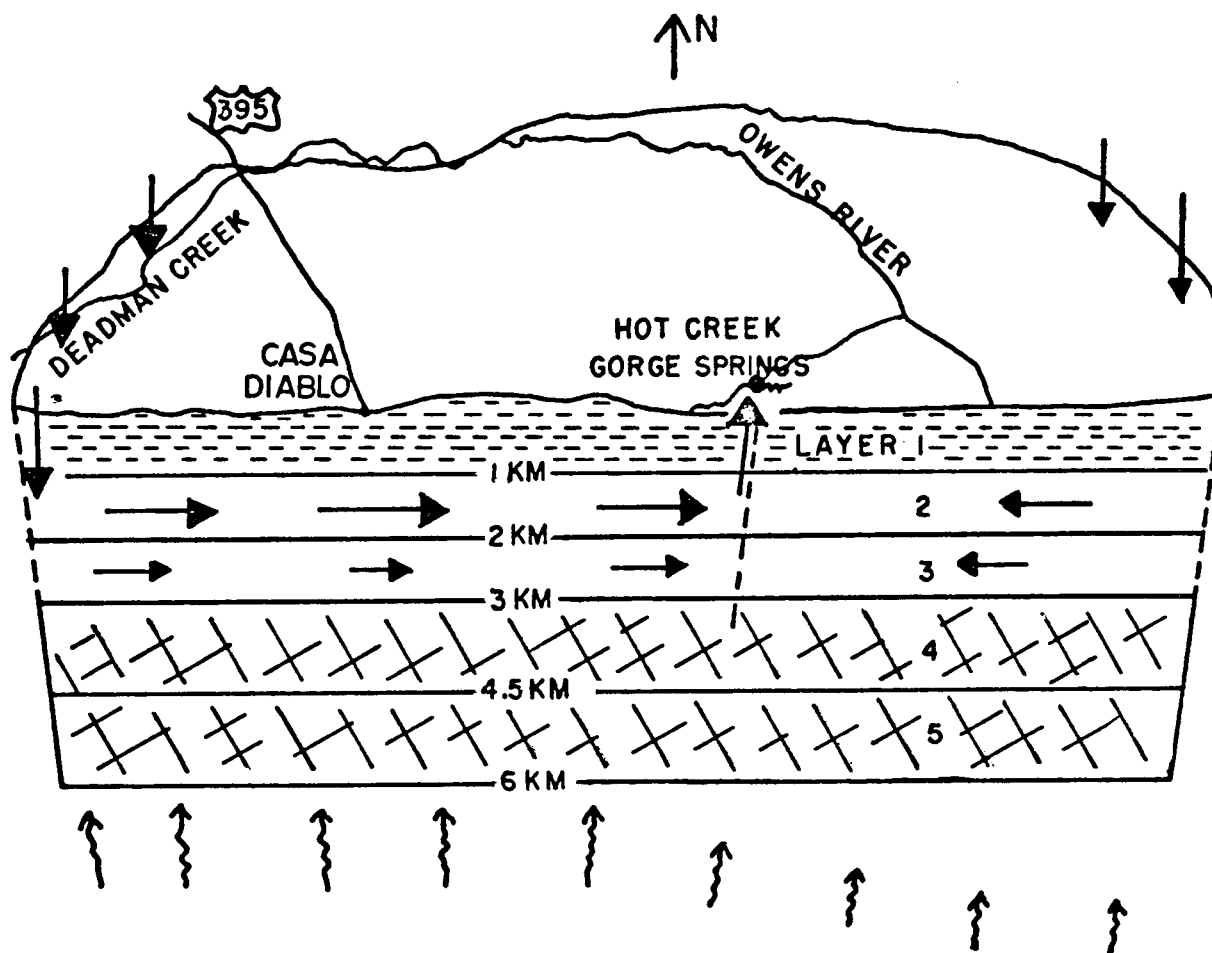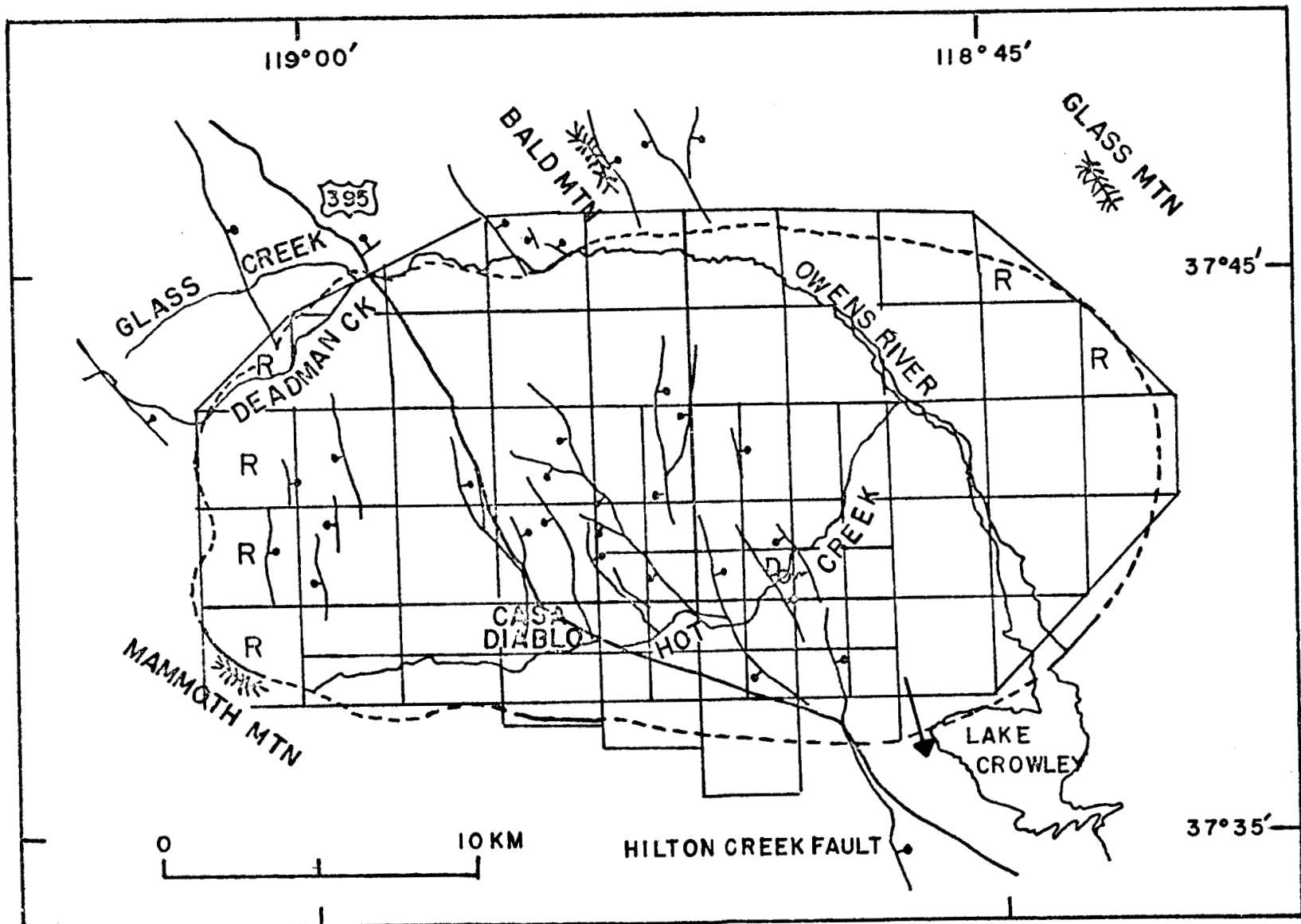other points of reference.

Figure 2. Block diagram showing conceptual model of Long Valley
hydrothermal system.

System consists of five horizontal layers having
properties listed in text. Patternless layers between
depths of 1 and 3 km represent hydrothermal reservoir
in fractured, densely welded Bishop Tuff. Recharge to
the reservoir is by way of the caldera ring fault in
the west and northeast. Discharge is by way of faults
and fractures to springs in Hot Creek gorge. Straight
arrows indicate ground-water flow; wavy arrows indicate
heat flow.

Figure 3.   Sketch map of Long Valley caldera showing nodal configuration for numerical simulation of hydrothermal model with uniform reservoir permeability distribution.   R denotes recharge node; D denotes discharge node covering Hot Creek gorge.   Principal faults are shown as solid heavy lines with ball on downthrown side.   Arrow denotes discharge at depth through southeastern caldera rim.
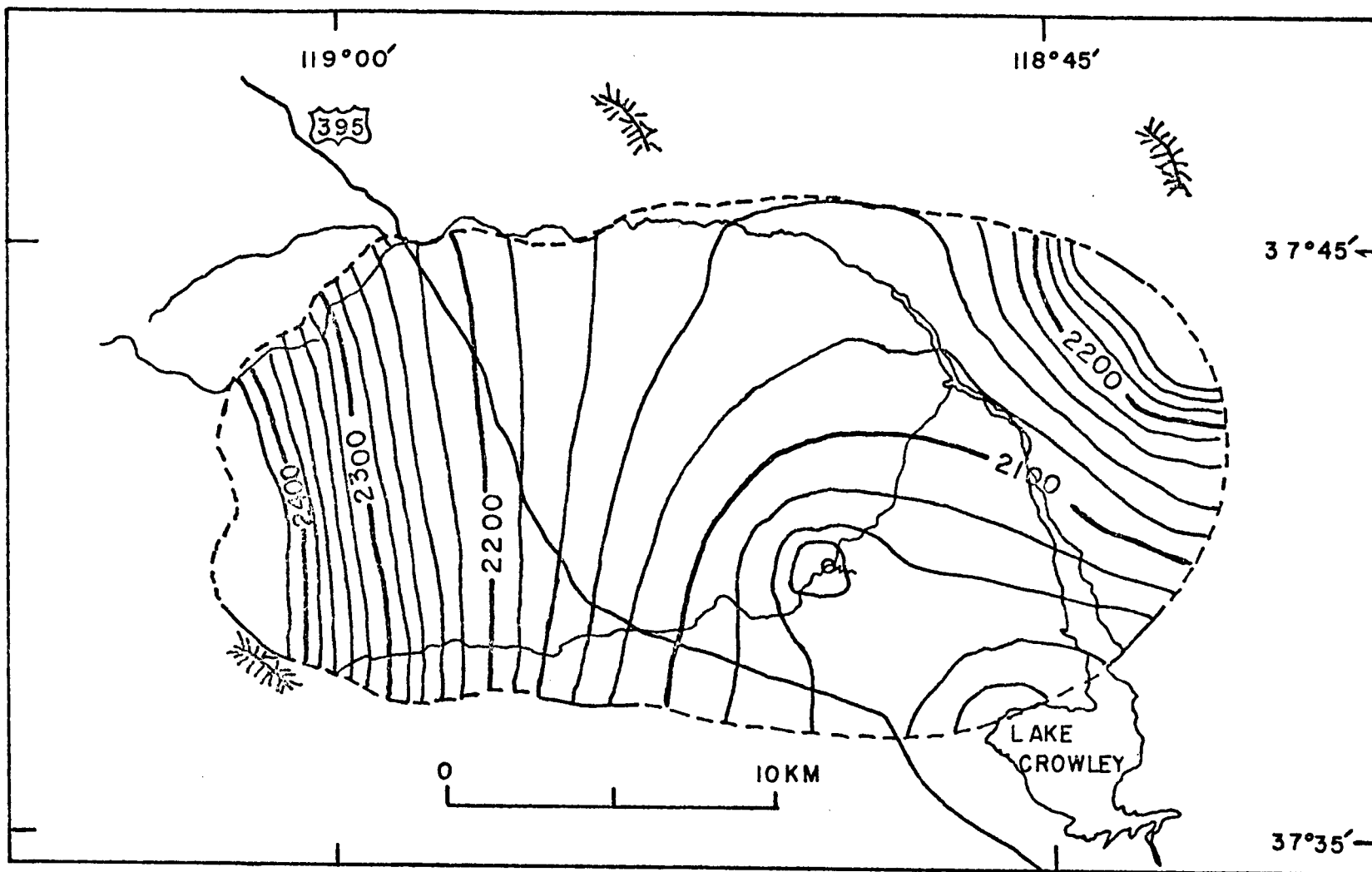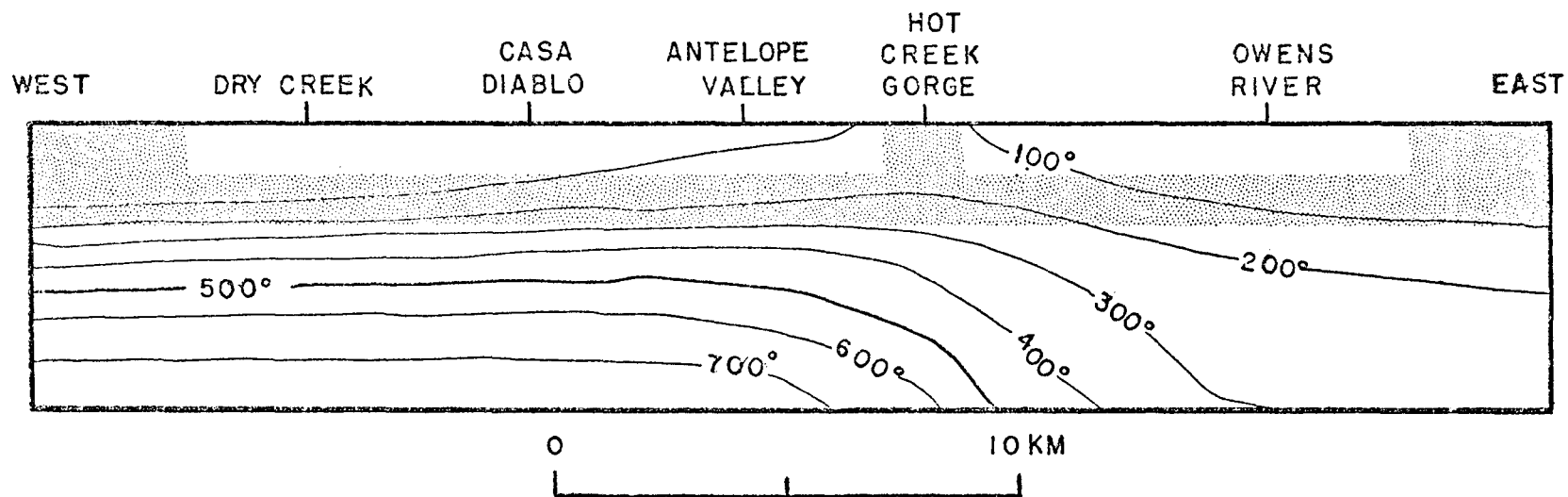
Figure 4. Sketch map of Long Valley caldera showing equivalent hydraulic head at a depth of 1.5 km in reservoir with uniform reservoir permeability of 30 millidarcys, hot-spring discharge of 250 kg/s, and southeast-rim outflow of 110 kg/s. Contours of equivalent hydraulic head in meters above mean sea level. Interval 20 m.

Figure 5. Diagrammatic east-west cross-section of Long Valley caldera showing isotherms in model after 35,000 years with hot-spring discharge of 250 kg/s, southeast-rim outflow of 110 kg/s, and reservoir depth of 1-2 km.

HOT
CASA ANTELOPE CREEK OWENS
WEST DRY CREEK DIABLO VALLEY GORGE RIVER EAST
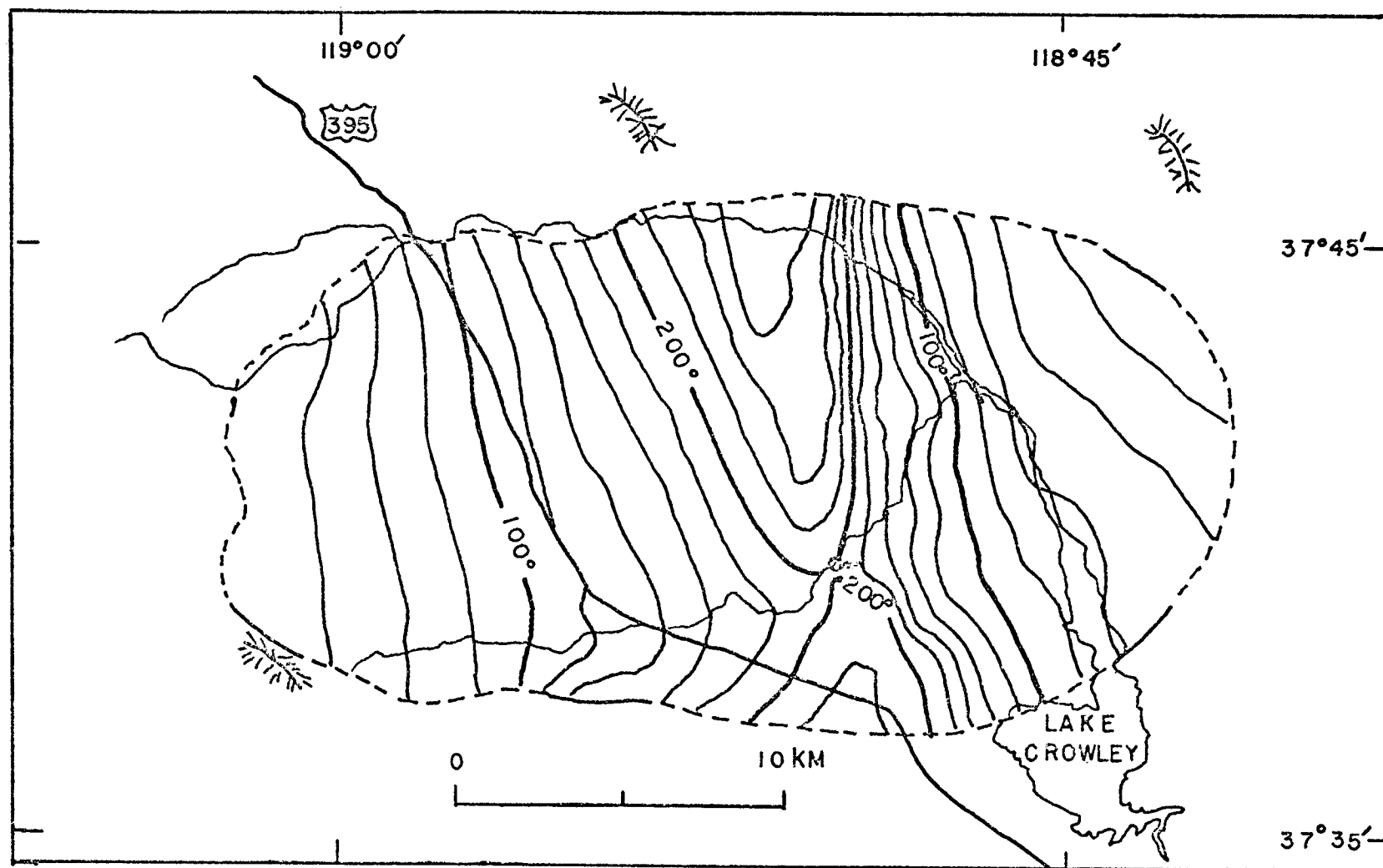
100°
200°
500° 300°
400°
700° 600°

0 10 KM

Figure 6. Sketch map of Long Valley caldera showing isotherms at a depth of 1.5 km in reservoir after 35,000 years with hot-spring discharge of 250 kg/s and southeast-rim outflow of 110 kg/s. Lines of equal temperature in degrees Celsius. Interval 20°C.

Figure 7. Transient response since initiation of springflow of average reservoir temperature below Hot Creek gorge for two simulated reservoir depths.